AIAA 93-0446

BLOWOUT AND LIFTOFF LIMITS OF A HYDROGEN JET FLAME IN A SUPERSONIC, HEATED, COFLOWING AIR STREAM

Youngbin Yoon, Jeffrey M. Donbar and James F. Driscoll

Department of Aerospace Engineering
University of Michigan, Ann Arbor MI

31st Aerospace Sciences Meeting & Exhibit
January 11-14, 1993 / Reno, NV

BLOWOUT AND LIFTOFF LIMITS OF A HYDROGEN JET FLAME IN A SUPERSONIC, HEATED, COFLOWING AIR STREAM

Youngbin Yoon, Jeffrey M. Donbar* and James F. Driscoll**

Dept. of Aerospace Engineering, Univ. of Michigan, Ann Arbor MI 48109

Abstract

Flame blowout limits have been measured for the case of a hydrogen jet flame surrounded by a heated, supersonic, coflowing air stream. The stagnation temperature of the Mach 2.0 air stream was varied from 294 K up to the autoignition temperature of 900 K; hydrogen injection velocities were varied up to 1300 m/s. It was found that the flame blowout curves display two distinct stable regions which are bounded by the: (a) far-field blowout limit and (b) near-field blowout limit. Far-field blowout occurs after a flame first lifts off and is associated with a sufficiently large fuel velocity; the shape of the far-field blowout curve can be explained by previous lifted flame analyses. Near-field blowout is a sudden blowout which occurs after no liftoff, and requires a sufficiently large air velocity. Current analyses have yet to explain the near-field limits.

The present measurements show how to select parameters in order to extend the stable region of the near-field blowout limit curve so that it extends into the regime of supersonic air velocities. Supersonic flame stability requires sufficient stagnation temperature, fuel tube outer diameter and fuel tube lip thickness. The improved stability due to elevated stagnation temperature can be explained by the temperature dependence of the chemical reaction rate. Air density also is shown to be important since it is the momentum of the air stream that determines how the velocity profile and stoichiometric profiles overlap. Also quantified were other parameters that are needed to model the flame stabilization process, including the flame liftoff distance and the flame length.

** Corresponding author: Prof. J.F. Driscoll, (313) 936-0101, Fax: (313) 763-0578

* U.S.A.F. Palace Knight Graduate Research Assistant

Introduction

The purpose of the present work is to quantify the fairly narrow range of conditions that allow a hydrogen jet flame to be stabilized in a coflowing supersonic air stream. It was decided to use a simple geometry (a fuel jet surrounded by a coflowing air stream) because the boundary conditions are most appropriate for numerical modelling of the flame blowout problem. It also was decided to operate a relatively small facility, as described below, having a supersonic test section with an inlet area of 14 cm^2, an exit area of 45 cm^2 and a length of 55 cm. It is argued that the trends reported herein are of a general, facility-independent nature because the physics of the type of flame stabilization process that is studied depend only on the near-field flow pattern in the 2-3 cm region just downstream of the fuel tube exit. In fact, it is shown below that the flame blowout limits did not change significantly even when the supersonic test section walls were removed entirely.

The physics of the flame blowout problem are sufficiently well known to explain the general flame stability diagram shown in Fig. 1. This schematic diagram summarizes measurements made for relatively low-speed fuel jets injected into subsonic coflowing air streams [1-7]. There are two mechanisms that lead to the blowout of non-premixed jet flames: (a) far-field blowout of a lifted flame, which is characterized by the limit (a) that is plotted in Fig. 1, and (b) near-field blowout, which occurs suddenly and with no liftoff and is characterized by the limit denoted (b) in Fig.1.

It is the near-field blowout limit that is of interest in the present study. Note that the near-field limit in Fig. 1 occurs when the fuel flowrate is relatively small compared to the air flowrate, (ie., stoichiometric or less) which is characteristic of propulsion devices. The near-field blowout limit is a lobed-shaped curve that can extend far to the right (ie. to large air velocities) in Fig. 1; the goal of the present work is to quantify some general ways to extend the near-field blowout limit into the supersonic air velocity regime. In general, the way to extend the near-field blowout limit curve to higher air velocities is to increase the air temperature, increase the fuel tube lip thickness, or to increase the fuel tube diameter, for reasons that are discussed below. Another way to significantly increase the near-field blowout limit is to add swirl to the air stream, as demonstrated in our laboratory [8] and in the ramjet experiment of Nejad et. al [9]. However, swirl was not considered in the present work.

The far-field blowout process has been analyzed using premixed flame concepts [10-12] since such flames are lifted prior to blowout and considerable premixing must occur in the liftoff region. Van Tiggelen [10] argues that the base of the flame will be stable at a location where the local turbulent (premixed) burning velocity equals the local gas velocity. His analysis and measurements [11,12] show that for the case of entrained air (no coflow velocity), the fuel velocity at blowout is:

$$U_F = c_1 \, d_F \, (S_L^2 / \alpha) \qquad (1)$$

The fuel jet diameter is d_F, S_L is the maximum laminar burning velocity, and α is the thermal diffusivity; the constant c_1 depends on fuel properties, including gas densities, the Prandtl number and the value of the stoichiometric mixture ratio. The uppermost point in the flame blowout curve shown in Fig. 1 has been found to be accurately predicted by Eq. 1. Physically, Eq. 1 is explained by the concept that the turbulent burning velocity of the base of a stable lifted flame is just balanced by local gas velocity; increasing U_F increases the local gas velocity, which is destabilizing; increasing S_L increases the burning velocity,

which is stabilizing. Larger jet diameter d_F lengthens the flame so that the longer stoichiometric contour overlaps lower velocity and lower strain regions downstream, which is stabilizing. The nonlinear dependence of S_L arises from the nonlinear formula for turbulent burning velocity used in Ref. 11. When coflowing air is used, the analyses of Refs. 4 and 5 include the air stream momentum to determine the gas velocity near the base of the lifted flame in the far field.

It is seen in Fig. 1 that from any stable condition just to the left of curve (a), one can blow out the flame by either increasing or by sufficiently decreasing the fuel velocity. The excessive fuel velocity limit is explained by the competition between burning velocity and gas velocity that was described above. Decreasing the fuel velocity leads to instability because the flame becomes shorter with coaxial air present. The gas velocity in the downstream region of the stoichiometric contour remains relatively large because of the coaxial air, therefore there no longer exists a sufficiently low velocity region near the stoichiometric contour at which the base of the lifted flame can stabilize.

The near-field blowout limit (region (b) in Fig. 1), which is the focus of the present work, cannot be modelled by the premixed analysis above because the stable flame is attached and insignificant premixing is believed to occur upstream of the flame base. Instead, stability is believed to occur if the instantaneous stoichiometric contour overlaps a region of sufficiently low velocity such that the diffusion flame is not strained out [13]. Figure 2 illustrates the overlap of the stoichiometric contour and the low velocity wake-like flow field behind the fuel tube. Turbulence models are available that can predict the mean velocity profiles, the mean stoichiometric contour, and the mean strain rate in terms of the scalar dissipation rate [13]; but to date the near-field blowout limit has not been predicted. An objective of the present work is to optimize the overlap of the stoichiometric contour and the low velocity region near the flame base, in order to increase the size of the stable region that is denoted region (b) in Fig. 1. The use of a thick fuel tube lip (ie. a bluff-body) [7] or swirl [8] increases the size of the low-velocity region and therefore can significantly extend the near-field stability curve to larger air velocities. No swirl is considered herein.

The four most important parameters that govern the near-field blowout process are:

$$U_F / U_A , \qquad d_o / d_i , \qquad \rho_F / \rho_A , \qquad (U_A / d_o) / (S_L^2 / \alpha) .$$

The first three parameters affect the location of the stoichiometric contour and the strain exerted on this contour. Subscripts F and A denote fuel and air averaged properties at the fuel injection location and the fuel tube outer and inner diameters are d_o and d_i. The fourth parameter is the inverse Damkohler number; it depends on the reaction rate associated with the particular fuel-air chemistry.

In addition to the above parameters, the wall confinement geometry was varied by considering two cases: flames confined within the test section described below, and flames for which the test section is removed and the supersonic air jet and flame expand into the laboratory. In the above list the Mach number is not included because it was held constant during supersonic operation since a single nozzle was used. The stagnation temperature of the air also is not included; it is argued that temperature effects are taken into account by the temperature dependence of the above reaction rate (S_L^2 / α) and by the temperature dependence of the above density ratio.

Experimental Configuration

A schematic of the University of Michigan Supersonic Combustion Tunnel is shown in Fig. 3. A 250 kW electrical resistance heater is used to provide a high enthalpy air stream having stagnation temperatures up to 1100 K (1520 F). Electrical heating was used instead of using vitiated air from a combustion process because flame blowout is sensitive to the radicals which are present in unknown concentrations in vitiated air. The settling chamber is 10.82 cm (4.26 in.) in diameter; stagnation pressures are varied up to 130 psia. The Mach 2 nozzle is two-dimensional, having a width of 4.06 cm and a length of 10.16 cm; the method of characteristics was used to design the contoured sidewalls [14]. The combustor test section has two sidewalls that are parallel and separated by 4.06 cm. The other two sidewalls each have a divergence angle (that equals the test section divergence half-angle) that can be varied from zero to six degrees but was set to four degrees for the present study. Proper sidewall divergence is required to prevent thermal choking and to maintain a constant Mach number in a supersonic stream with heat addition. The combustor length is 55 cm (21.7in) and the combustor inlet heigth is 3.45 cm. The combustor outlet heigth is 11.2 cm for the 4 degree test section divergence half-angle used. All components are made of stainless steel. The diffuser wall is water cooled. Eight static pressure taps are located at equally spaced intervals. Eight Vycor glass windows provide optical access for imaging diagnostics.

Various fuel tubes having different inside and outside diameters are mounted on the tunnel centerline to provide hydrogen at 294 K. The fuel nozzle exit is 16 cm downstream of the end of the supersonic air nozzle. The fuel and the air mass flowrates are monitored using calibrated choked orifices. An ignitor port is located 2 cm downstream of the fuel nozzle. When the flame was operated in the unconfined mode, the test section was removed and the Mach two nozzle described above was replaced with a Mach two axisymmetric nozzle which had a throat area that was 45% larger than the original nozzle. Some descriptions of combustors used in previous supersonic flame studies are given in Refs. 15-23.

Results (a) - Flame Photographs and Air Stream Properties

A direct photograph of the hydrogen jet flame in the unconfined supersonic airstream is shown in Fig. 4. The flame length is 47 d_j , where d_j is 0.64 cm. This flame length is considerably less than that of a turbulent hydrogen jet flame in ambient air, which is 150 d_j, because air is forced into the flame shown in Fig. 4. It is interesting to note that the flame in Fig. 4 has a narrow neck region just downstream of the stabilization location, ie., it does not have the same shape as a jet diffusion flame with no coflow. The neck region is believed to be due to the high strain exerted on the flame by the air stream; the flame appears to be brighter in the region upstream of the neck, which is a region of relatively low velocity in the wake of the fuel tube. The neck region has relatively little flame radiation and appears to be on the verge of local flame extinction.

A photograph of the base of the confined supersonic flame is shown in Fig. 5 The flame is observed to be locally extinguished immediately downstream of the fuel nozzle exit, which is the inner circle seen in Fig. 5. Instead, the flame is stabilized at a location near the outer edge of the bluff body. The stoichiometric contour begins at the fuel nozzle exit and can be distorted by two recirculation zones that are driven by the fuel stream and the air stream, respectively, as has been shown by Chen and Driscoll [24]. Therefore, the unreacted fuel and air are in contact at the stoichiometric contour for a distance of several

fuel jet diameters before reaction occurs. The degree of molecular mixing of fuel and air during this igniton delay time is not known, but the degree of mixing may greatly influence whether the resulting flame is similar to a premixed or a nonpremixed strained flame. Previous work by Roquemore, et al. [25] also showed how a bluff-body flame is stabilized at the outer edge of the bluff-body and not at the fuel nozzle exit. The flame tip is not shown in Fig. 5; for this confined flame the tip is open in that the maximum axial location of flame radiation occurs near the walls (similar to a rod-stabilized premixed flame) and not near the centerline. The unconfined flame has a closed flame tip such that the maximum location of flame radiation occurs on centerline, similar to a jet diffusion flame.

The wall static pressure measurements that are shown in Fig. 6 indicate that the supersonic flowfield in the combustor is shock-free and that the Mach number is nearly constant at all locations. With no flame (ϕ=0.0), the wall static pressure decreases in the axial direction, as expected, due to the combustor divergence half-angle of four degrees. Operating the flame at an overall equivalence ratio (ϕ) of 0.05 to 0.18 causes the static pressure to be larger than the static pressure with no flame, as expected, because heat addition decreases the Mach number and increases the static pressure. The four degree wall divergence was chosen because it provides a static pressure decrease with axial distance that just counteracts the static pressure rise with axial distance associated with heat release. Therefore the upper four curves in Fig. 6 do not vary appreciably in the axial direction and the Mach number is 1.9, to an accuracy of plus or minus 0.1.

Results (b) - How Blowout Limits Scale With Fuel Tube Outer Diameter

Figures 7 and 8 shows some typical near-field flame blowout limits that were measured for the confined and the unconfined flames, respectively. The shapes of these curves are similar to the schematic that appeared in Fig.1. In addition, some far-field limits of the unconfined flame are shown in Fig. 8; similar lifted flames were not obtained in the confined geometry and are not shown in Fig.7 because of limitations to the hydrogen fuel flowrates. The hydrogen mass weighted velocity (U_F) that is plotted is defined as $\rho_F U_F/\rho_{F,stp}$ where U_F is the fuel velocity and $\rho_{F,stp}$ is the fuel density at 298K and 1 atm. The quantity $\rho_F U_F$ was measured by dividing the measured fuel mass flow rate by the fuel tube area ($\pi d_i^2/4$). The air mass weighted velocity (U_A) is defined in a similar manner. Figures 7 and 8 show that the mass weighted air velocity is the relevant parameter, rather than the air velocity alone. After Mach 1.9 conditions are achieved, the Mach number and the air velocity remains constant, yet further increases in the air mass flowrate (ie. increases in ρ_A) lead to flame blowout. Therefore flame blowout and the contours of gas velocity and stoichiometry that were shown in Fig.2 depend on both the gas velocity and the gas density, as expected. However a detailed model is needed to show how an increase in the air stream density (ie., air stream momentum) distorts the velocity profiles and the stoichiometric contour in such a way that the flame is destabilized.

Both Figures 7 and 8 indicate that improved stability is achieved by increasing the outer diameter of the fuel tube, while maintaining a constant inner diameter. The larger fuel tube rim thickness creates a larger bluff-body recirculation zone, which allows the stoichiometric contour to overlap a low velocity region, as was shown in Fig. 2. It also is seen that the far-field blowout curve in Fig. 8 is not affected by variations in d_o, as expected; all the data obtained for U_F above 1100 m/s collapse to a single curve.

The effect of wall confinement is deduced by comparing Fig.7 to Fig. 8. The maximum air velocities associated with each of the curves is approximately the same for the confined flames (Fig.7) and the unconfined flames (Fig.8). The major difference is that the confined flames are more stable and do not lift off at fuel velocities above 1000 m/s, as do the unconfined flames. The reasons for this difference is not yet known; however the flowfields differ in that the unconfined flame exists in a supersonic flow downstream of an overexpanded nozzle, which consists of a diamond-shaped plume of oblique shock waves and expansion fans, whereas the confined flowfield is shock-free.

Results (c) - Effects of Varying the Air Stagnation Temperature

It was decided to quantify the expected improvement in the flame stability as the air stagnation temperature was increased from 294 K up to the autoignition temperature of 900 K. Existing theories that apply for near-field blowout (ie., strained diffusion flames[13, 26]) and for the far-field blowout (of lifted, partially premixed flames[4,10-12]) predict that an increased gas temperature will increase the flame stability limits by the factor (S_L^2/α), where the temperature sensitivity of the laminar burning velocity S_L is known. Figures 9 and 10 show that the maximum air velocity at which the flame is stable can be increased by a factor of ten (from a minimum of 60 m/s to a maximum of 600 m/s) by increasing the air stagnation temperature. The air velocity in Figs. 9 and 10 is weighted by the density ratio ρ/ρ_{T_o} where ρ_{T_o} is the reference gas density at 1 atm and the particular stagnation temperature. Autoignition was observed in some instances when T_{oA} was 900K.

Results (d) - Comparison to Previous Subsonic Flame Studies

Some comparisons of the present results to previous work that was conducted in a lower air velocity range are shown in Fig. 11. For comparison purposes, the present flames were made less stable than for the above cases by using a thin fuel tube lip (d_o-d_i) equal to 0.10 cm. and by setting T_o equal to 294 K. Vranos [2] reported subsonic hydrogen flame blowout limits for similar conditions and his results are in reasonable agreement with the present trends that appear in Fig. 11. Takahashi [3] reports hydrogen flame blowout limits for lip thicknesses that are significantly smaller than those used herein; his near-field blowout curve shown in Fig. 11 does not extend to air velocities that are as large as those illustrated by the other curves shown, which is expected.

The flame liftoff height is another parameter that can be used to assess the validity of flame stability models; some typical liftoff heights are shown in Fig 12 for the high fuel velocities (up to 1248 m/s) that were used in the present work. At present there is no general model that predicts liftoff heights when coflowing air is used, but analysis of a jet flame with no coflowing is reported in Ref.13. This model is based on the idea that the flame base lifts off to a location where the local strain rate is sufficiently low such that the non-dimensional scalar dissipation rate, which could be computed using a k-epsilon code, equals a critical, universal value. Figure 12 indicates that the liftoff height is nearly a linear function of the air velocity. The increased air velocity exerts strain on the flame base, which increases the liftoff height. The increased air that is forced into the fuel jet also causes the stoichiometric contour to move radially inward where the jet velocities are maximum, which can explain the positive slope seen in Fig. 12. As the stagnation temperature of the air is increased to 600K, Fig. 13 shows that approximately twice the air velocity is required to lift off the flame for the heated air conditions (solid symbols) than for the unheated air conditions (open symbols).

The visible lengths of the hydrogen-air flames were measured since flame length is a parameter that affects the far-field flame blowout limit. Flame length indicates the overall

rate that air is entrained into the flame. In a short jet flame, most of the flame experiences relatively high velocity and high strain rate, while in a long flame there is a downstream region where there is a stoichiometric region where a low strain rate occurs, and the flame can lift to such a region. Flame lengths shown in Fig. 14 increases linearly with the fuel flow rate, which is characteristic of flames having a coflowing airstream. In contrast, a turbulent jet diffusion flame with no coflow has a length that is constant and is independent of fuel flowrate. For such a flame, increasing the fuel flowrate causes a corresponding increase in the fuel-air mixing rate so the flame length remains constant. The flame length does not remain constant in Fig. 14 because the fuel-air mixing rate is determined by the airflow velocity, which is constant, rather than the fuel velocity. Therefore an increase in the fuel flowrate (with a constant mixing rate) results in the longer flame, which explains the trends seen in Fig. 14.

It is noted that the lengths of the confined flames (closed symbols in Fig.14) are equal to the lengths of the unconfined flames (open symbols), but this result may be coincidental. The unconfined flame experiences numerous weak shock waves and expansion waves in the diamond-shaped overexpanded plume and these waves are expected to affect the fuel-air mixing process. However, the effects of these waves on the gas velocity may be compensated by the opposite effects of the waves on the gas density.

Before a conclusive model can be developed to predict the type of flame blowout limits presented herein, several local measurements are suggested. It is planned to obtain images of the instantaneous velocity profile, the flame location (from OH imaging) and the scalar dissipation rate, which is a measure of the strain exerted on the flame. Chen and Nejad [27] have developed a method to obtain the velocity profile near the base of a supersonic flame using OH-Flow-Tagging Velocimetry. Velocity profiles downstream of their Mach 2 fuel injector were imaged. Namazian, et al [28], Dahm and Buch [29] and Feikema and Driscoll [30] have measured the scalar dissipation rate in jet flows using Planar Rayleigh Scattering Imaging. The conserved scalar was imaged and the spatial derivative was computed in order to obtain instantaneous images of the scalar dissipation rate at the location where the flame would be stabilized.

Conclusions

1. Hydrogen jet flames could be stabilized in a supersonic airflow; as the mass-weighted air velocity is increased, the flames exhibited sudden near-field blowout without lifting off. The complete supersonic flame blowout curve displayed a trend that is similar to subsonic near-field blowout limit curves.

2. To extend the near-field blowout limit to supersonic airflows, the critical values of fuel tube lip thickness and air stagnation temperature are quantified.

3. Flame attachment occurs at the outer edge of the bluff-body fuel tube and not near the inner diameter where the fuel first exits the tube at velocities typically exceeding 1000 m/s. Some local extinction occurs for even the most stable, attached flames.

4. Flame liftoff height scales linearly with coflow air velocity and is independent of fuel tube outer diameter. The lengths of the supersonic flames increase linearly with fuel velocity, as is expected for flames with coflowing air.

5. Removing the combustor walls entirely did not significantly change the maximum air velocity at blowout for a range of fuel nozzle sizes, which indicates that blowout depends primarily on the local near-field conditions just downstream of the fuel nozzle.

Acknowledgement

Support for one of the authors (J. Donbar) was made possible by the U.S. Air Force Palace Knights Program; his mentor is Dr. A. S. Nejad of The Advanced Propulsion Division, Aero Propulsion and Power Laboratory, Wright-Patterson AFB OH 45433. The support of the University of Michigan also is acknowledged.

References

1. Feikema, D., Chen, R.-H., and Driscoll, J.F., "Blowout of Non-Premixed Flames: Maximum Coaxial Air Velocities Achievable, With and Without Swirl", Combust. Flame 86: 347-358, 1991.

2. Vranos, A., Taback, E.D., and Shipman, C.W.,"An Experimental Study of the Stability of Hydrogen-Air Diffusion Flames", Combust. Flame 12: 253-260, 1968.

3. Takahashi, F., Mizomoto, M., Ikai, S., and Tsuruyama, K., "Stability Limits of Hydrogen/Air Coflow Jet Diffusion Flames:, AIAA Paper 90-0034, 1990.

4. Dahm, W.J.A, and Mayman, A. G., "Blowout Limits of Turbulent Jet Diffusion Flames for Arbitrary Source Conditions", AIAA J. 28: 1157-1162, 1990.

5. Dahm, W.J.A., and Dibble, R.W.,"Combustion Stability Limits of Coflowing Turbulent Jet Diffusion Flames", Twenty-Second Symposium (International) on Combustion, The Combustion Institute, Pittsburgh, p.801, 1988.

6. Takeno, T., and Kotani, Y., "An Experimental Study of the Stability of a Jet Diffusion Flame", Acta Astron. 2: 999-1008, 1975.

7. Masri, A.R., and Bilger, R.W., "Turbulent Diffusion Flames Stabilized on a Bluff Body", Twentieth Symp. on Combust., The Comb. Inst., p.319-326, 1984.

8. Feikema, D., Chen, R.-H., and Driscoll, J.F.,"Enhancement of Flame Blowout Limits by the Use of Swirl", Combust. Flame 80: 183-195, 1990.

9. Nejad, A.S., Vanka, S.P., Favalaro, S. C., Sammimy, M., and Langenfeld, C., "Applications of Laser Velocimetry for Characterization of Confined Swirling Flows", J. of Engr. for Gas Turbines and Power 111: 36-45, 1989.

10. Vanquickenbourne, L., and van Tiggelen, A.,Combust. Flame 10: 59-68, 1966.

11. Kalghatgi, G., Combust. Sci. Technol. 26: 233-239, 1981.

12. Kalghatgi, G., Combust. Sci. Technol. 41:17, 1984.

13. Peters, N. and Williams, F.A., "Lift-Off Characteristics of Turbulent Jet Flames", AIAA J. 21: 423-429, 1983.

14. Shapiro, A.H., Compressible Fluid Flow, Ronald Press, New York, 1953.

15. Cookson, R.A., Flanagan, P. and Penny, G.S., Twelfth Symposium (International) on Combustion, The Combust. Inst., Pittsburgh, p.1115-1124, 1966.

16. Waltrup, P.J., Dugger, G.L., Billig, F.S., and Orth, R.C., "Direct Connect Tests of Hydrogen Fueled Supersonic Combustors", Sixteenth Symposium (International) on Combustion, The Comb. Inst., Pittsburgh, pp.549-556, 1976.

17. Northam, G.B., Trexler, C.A., and McClinton, C. "Flameholding Characteristics of a Swept Strut Hydrogen Fuel Injector for Scramjet Application, NASA TR-A81-10711, 1981.

18. Stull, F.D., "Scramjet Propulsion", AIAA Paper 89-5012, First National Aerospace Plane Conference, Dayton, July 1989.

19. Beach, H.L., "Supersonic Mixing and Combustion of a Hydrogen Jet in a Coaxial High-Temperature Test Gas", AIAA Paper 72-1179, 1972.

20. Kimura, I., Aoki, H., and Kato, M., "Use of a Plasma Jet for Flame Stabilization in Supersonic Air Flows", Combust. Flame 42: 297-305, 1981.

21. Drewry, J.E., "Supersonic Mixing and Combustion of Confined Coaxial Hydrogen-Air Streams", AIAA Paper 72-1178, Joint Propulsion Conference, Nov. 1972.

22. Stalker, R.J. and Morgan, R.G.,"Supersonic Hydrogen Combustion With a Short Thrust Nozzle", Combust. Flame 57:55-70, 1984.

23. Jacobs, P.A., Rogers, R.C., Weidner, E.H.,and Bittner, R.D."Flow Establishment in a Generic Scramjet Combustor", AIAA Paper 90-2096, 1990.

24. Chen, R.-H., Driscoll, J.F., Kelly, J., Namazian, M., and Schefer, R.W., "A Comparison of Bluff-Body and Swirl-Stabilized Flames", Comb.Sci.Technol. 71:197-217, 1990.

25. Roquemore, W.M., Reddy, V.K., Hedman, P. O., Post, M.E., Chen, T.H., Goss, L.P., Trump, D., Vilimpoc, V., and Sturgess, G.J., "Experimental and Theoretical Studies in a Gas Fueled Research Combustor", AIAA paper 91-0639, 1991.

26. Thevenin, D. and Candel, S., "Ignition Dynamics of a Diffusion Flame Rolled Up in a Vortex", Ecole Central de Paris internal report, submitted for publication.

27. Chen, T.H., Goss, L.P., Trump, D.D., Sarka, B., and Nejad, A. S., "The Effects of Nozzle Geometry Upon Sonic Fuel Injection As Studied By OH-Flow-Tagging Velocimetry", AIAA Paper 91-0575, AIAA Aerospace Sci. Meeting, 1991.

28. Namazian, M., Schefer, R.W., and Kelly, J.,"Scalar Dissipation Measurements in the Developing Region of a Jet", Combust. Flame 74:147-160, 1988.

29. Dahm, W.J.A. and Buch, K.A. "Fine Scale Structure of Conserved Scalar Mixing In Turbulent Flows. Part II: Sc=1", to appear in J. Fluid Mech., 1992.

30. Feikema, D. and Driscoll, J.F., "Scalar Dissipation Measurements at the Stabilization Location Near the Base of a Jet Diffusion Flame", Paper 38-1, Sixth Int'l Symp. on the Appl.of Laser Techniques to Fluid Mech., Lisbon, July 1992.

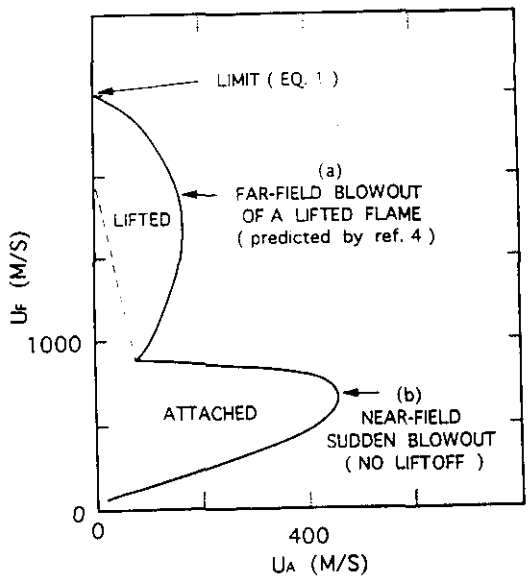

Figure 1. Schematic of the Stability Limits of a Non-Premixed Jet Flame That Is Surrounded by Coflowing Air. Note: the near-field limit (b) may not extend to large air velocities as shown unless the fuel tube lip is sufficiently thick.

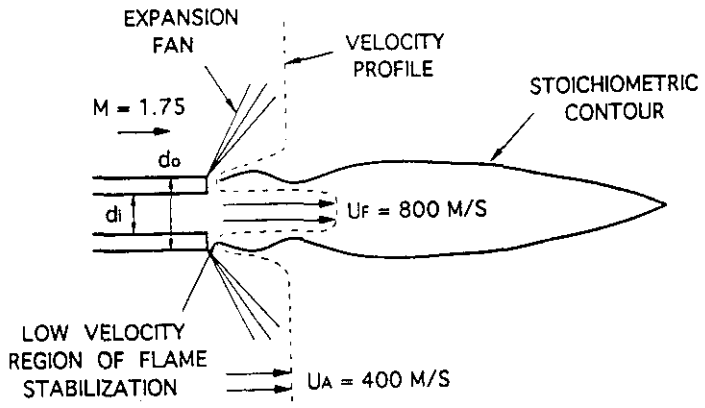

Figure 2. Schematic of Near-Field Flame Stabilization. Stabilization occurs where the instantaneous stoichiometric contour overlaps a sufficiently low velocity wake region.

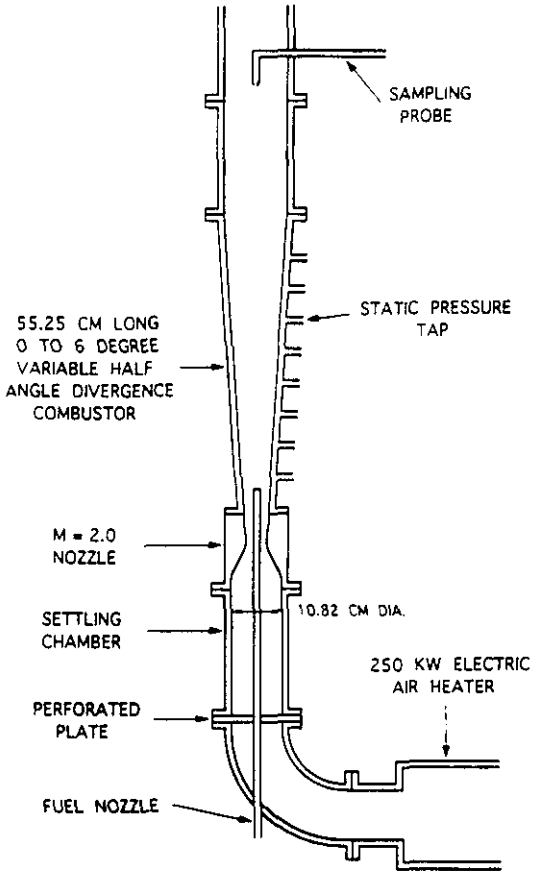

Figure 3. Schematic of the University of Michigan Supersonic High Enthalpy Combustion Tunnel.

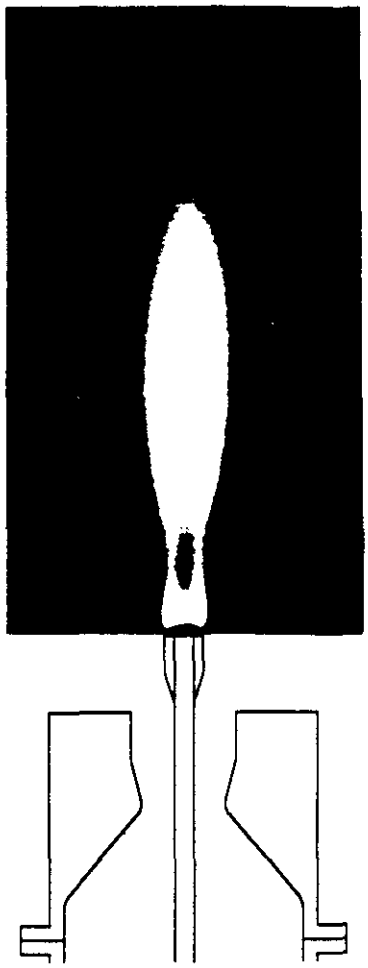

Figure 4 Direct Photograph of an Unconfined Supersonic Hydrogen-Air Flame. M_A =1.75, T_{oA}= 294 K, hydrogen mass weighted velocity = 862 m/s

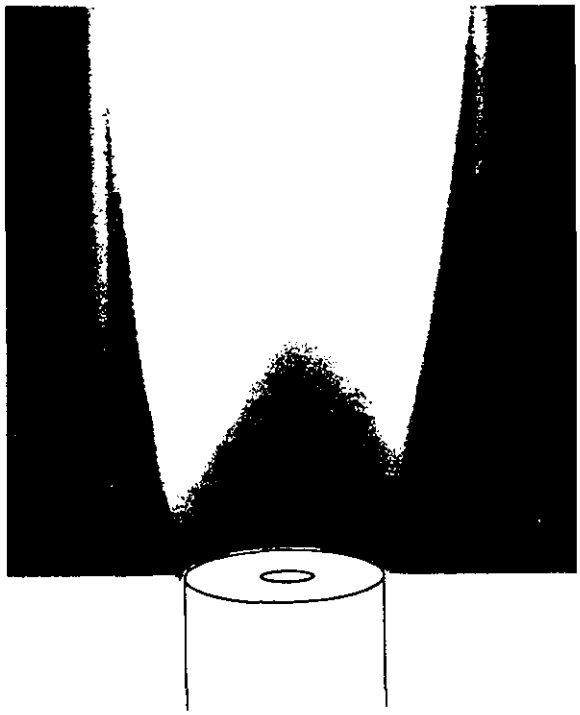

Figure 5. Direct Photograph of a Confined Supersonic Hydrogen-Air Flame. M_A=2.0, T_{OA}= 294 K, hydrogen mass weighted velocity = 764 m/s

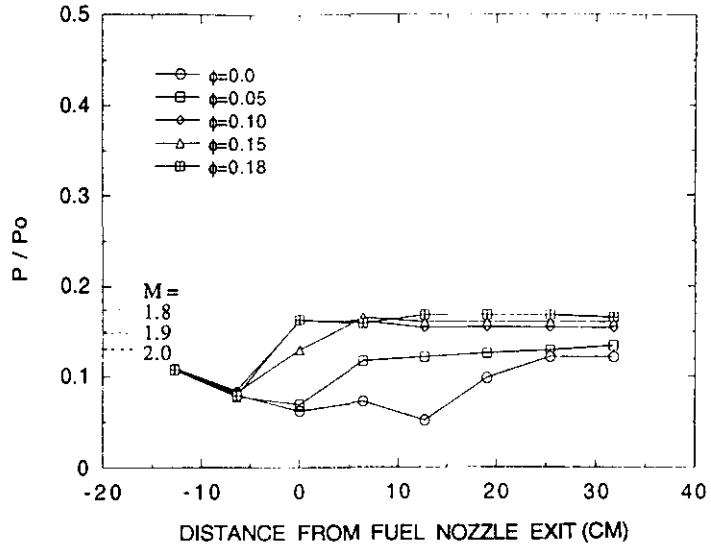

Figure 6. Wall Static Pressure Distribution in the Supersonic Combustor for Various Amounts of Heat Addition. Overall fuel-air equivalence ratio is ϕ. Local Mach number, deduced from pressure data above, exceeds 1.8 for all flame locations. P_o =94.7 psia, T_o= 294 K, d_o= 2.54 cm, d_i = 0.64 cm.

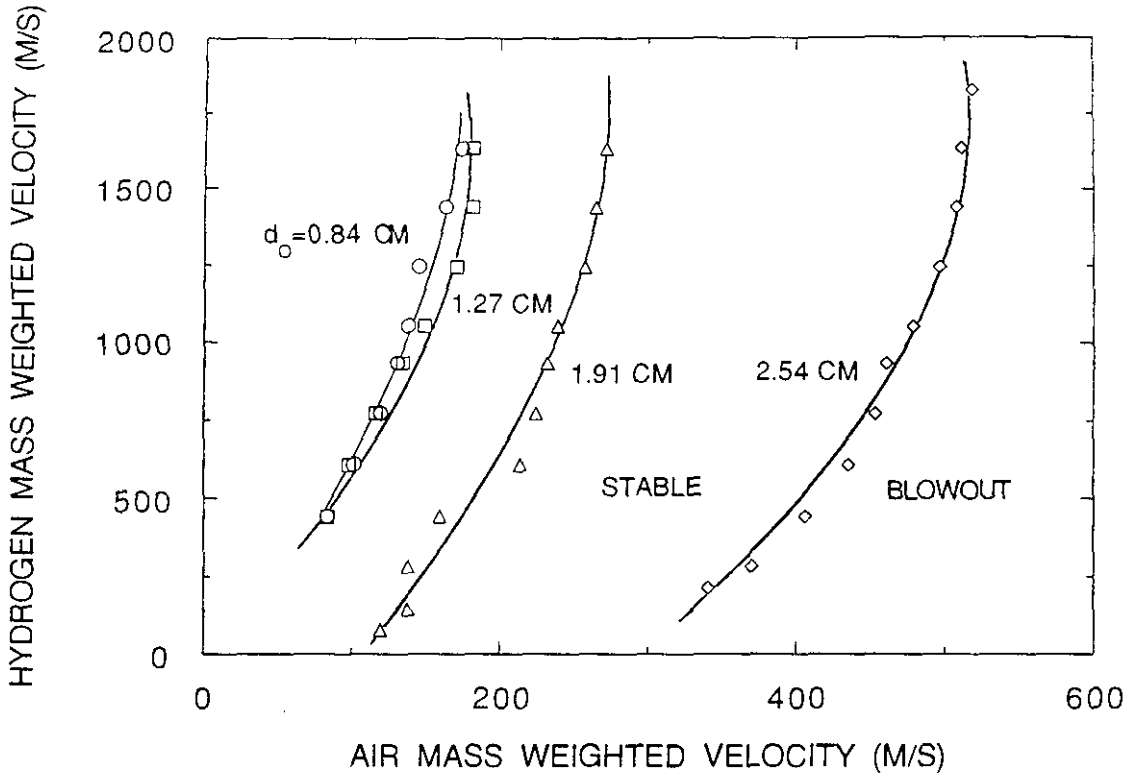

Figure 7. Effect of Varying the Fule Tube Outer Diameter (d_o) on the Blowout Limits of the Hydrogen-Air Flames. Case shown is confined. T_{OA} = 294 K, d_i = 0.64 cm.

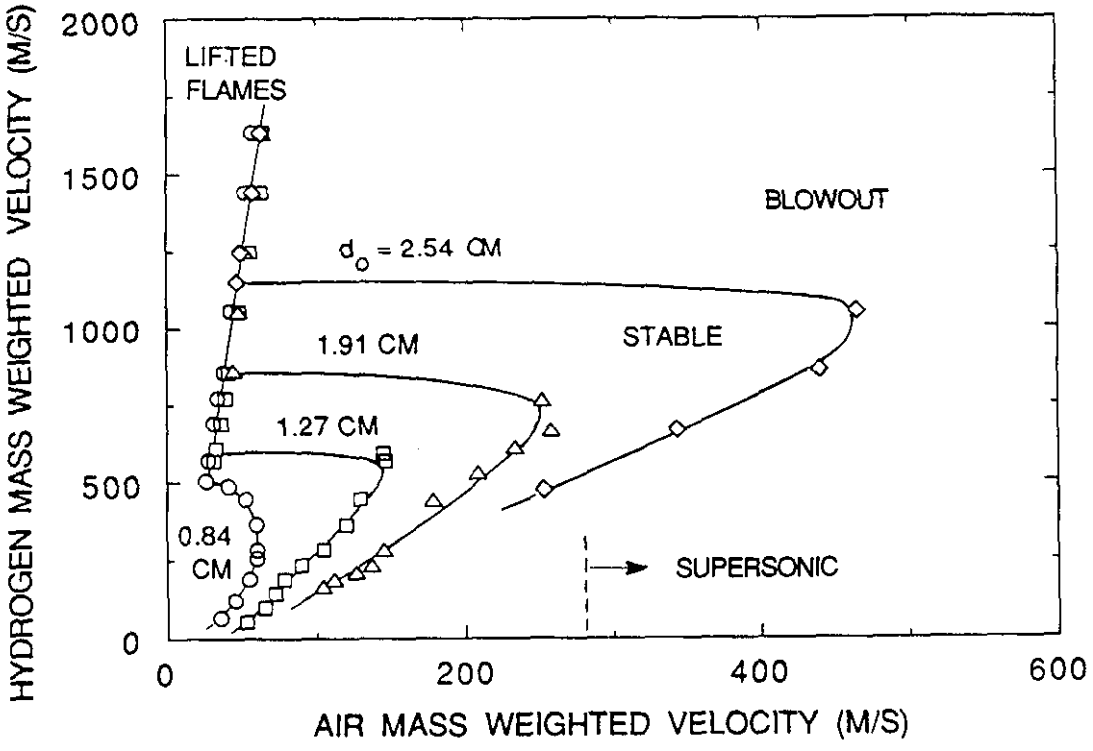

Figure 8. Effect of Varying the Fuel Tube Outer Diameter (d_o) on the Blowout Limits of the Hydrogen-Air Flames. Supersonic airflow occurs to the right of the dotted line. Case shown is unconfined. T_{OA} = 294 K, d_i = 0.64 cm.

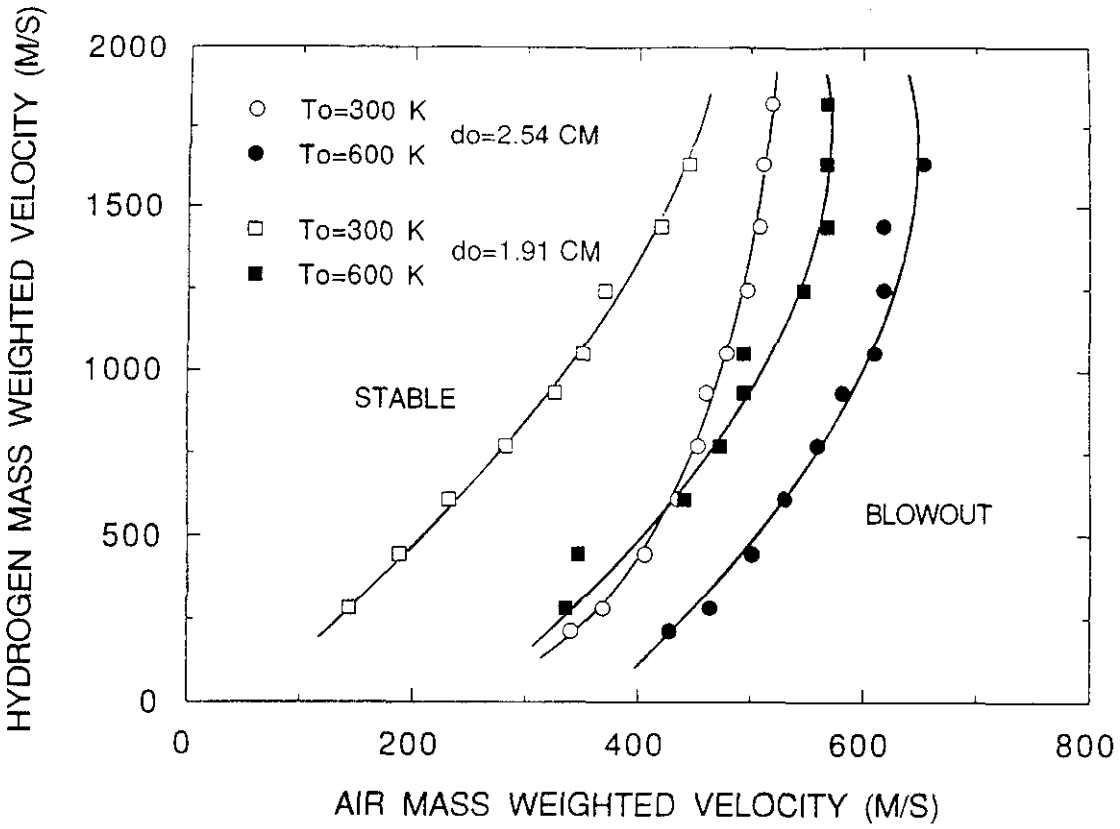

Figure 9. Air Stagnation Temperature Effects on Confined Flames; Temperatures Up To 600 K. d_o = 1.91 cm and 2.54 cm, d_i = 0.64 cm.

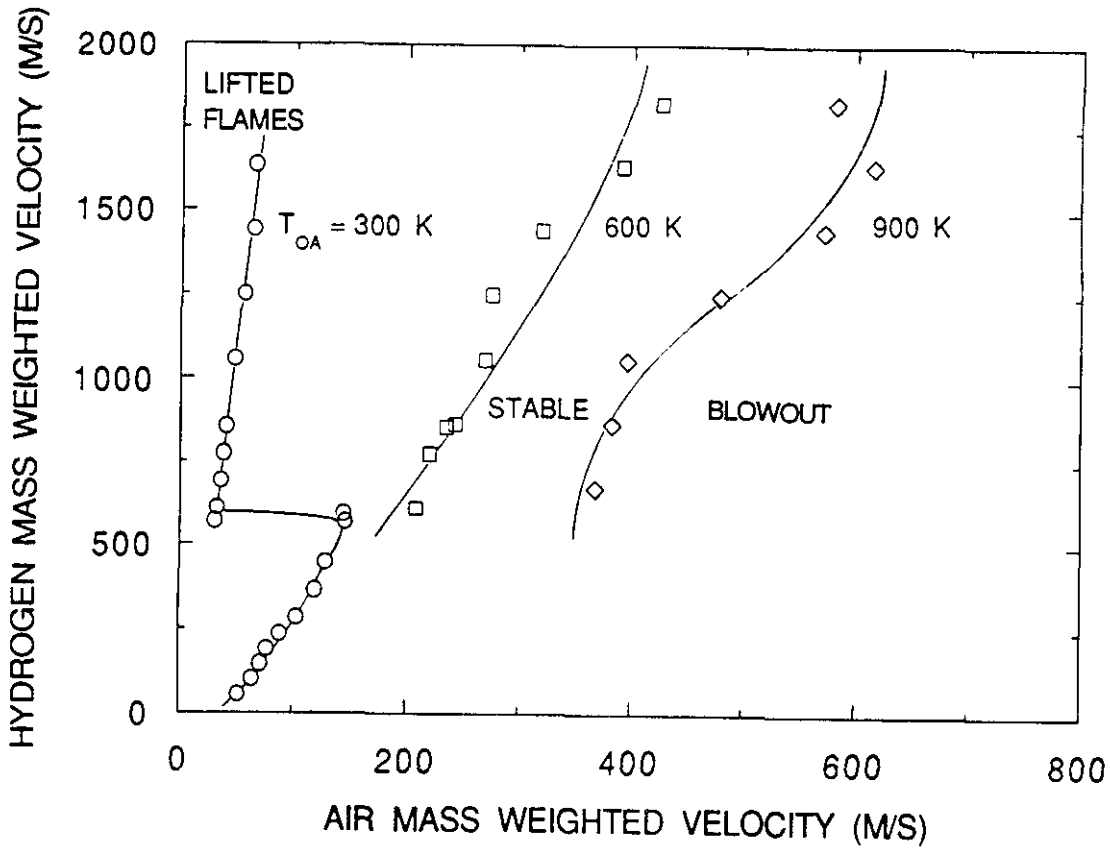

Figure 10 Air Stagnation Temperature Effects on Unconfined Flames; Temperatures Up To 900 K. d_o = 1.27 cm, d_i = 0.64 cm.

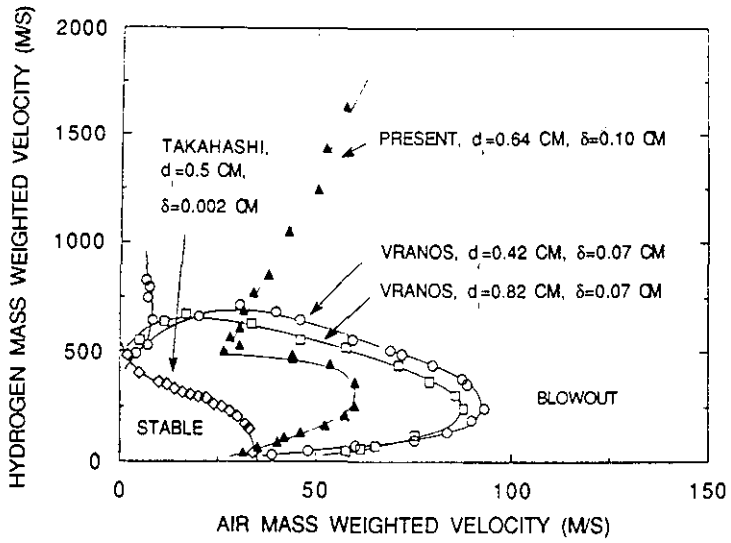

Figure 11 Comparison of Some Present Results to Previously Reported Blowout Limits of Hydrogen Flames in Subsonic Air Flows. All cases are unconfined

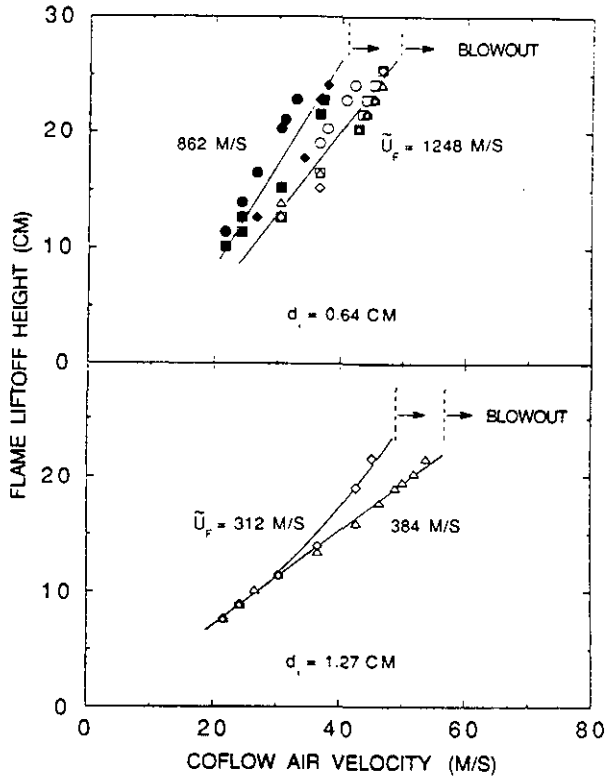

Figure 12 Flame Lift-Off Heights For Hydrogen Mass-Weighted Velocities of 862 and 1248 m/s. Sonic velocity of hydrogen is 1315 m/s. T_{oA} = 294 K.
d_o = ● ○ : 0.84 cm, ■ □ : 1.27 cm, ◆ ◇ : 1.91 cm, △ : 2.54 cm.

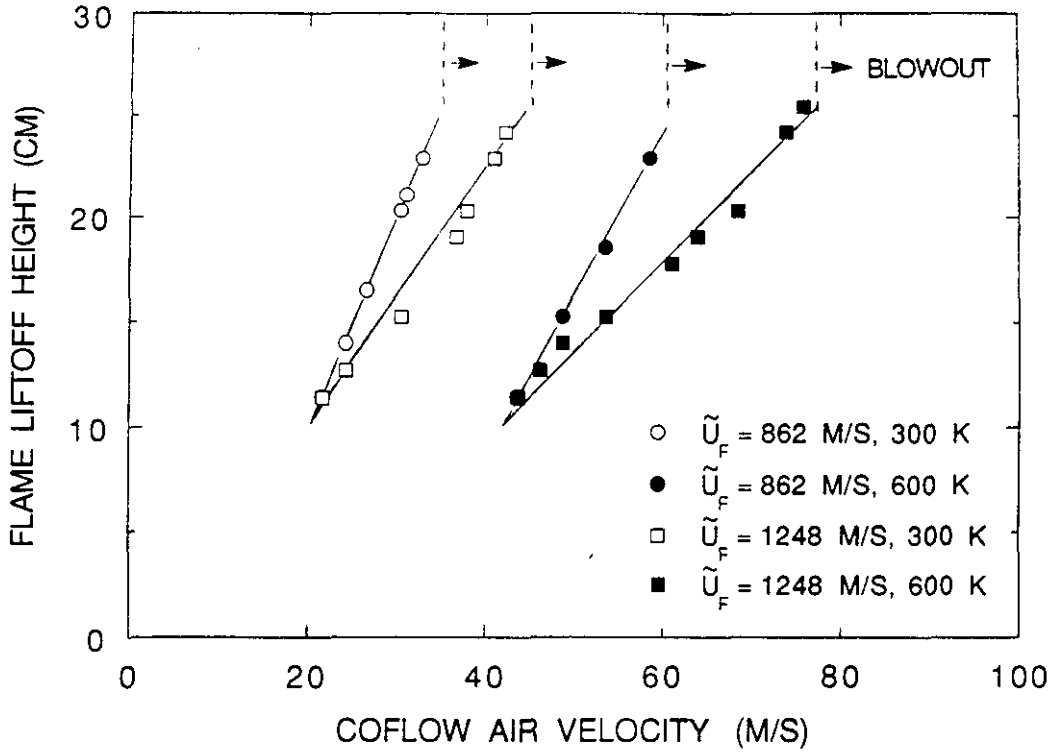

Figure 13 . Effect of Varying the Air Stagnation Temperature on the Flame Liftoff Height. d_o = 0.84 cm, d_i = 0.64 cm.

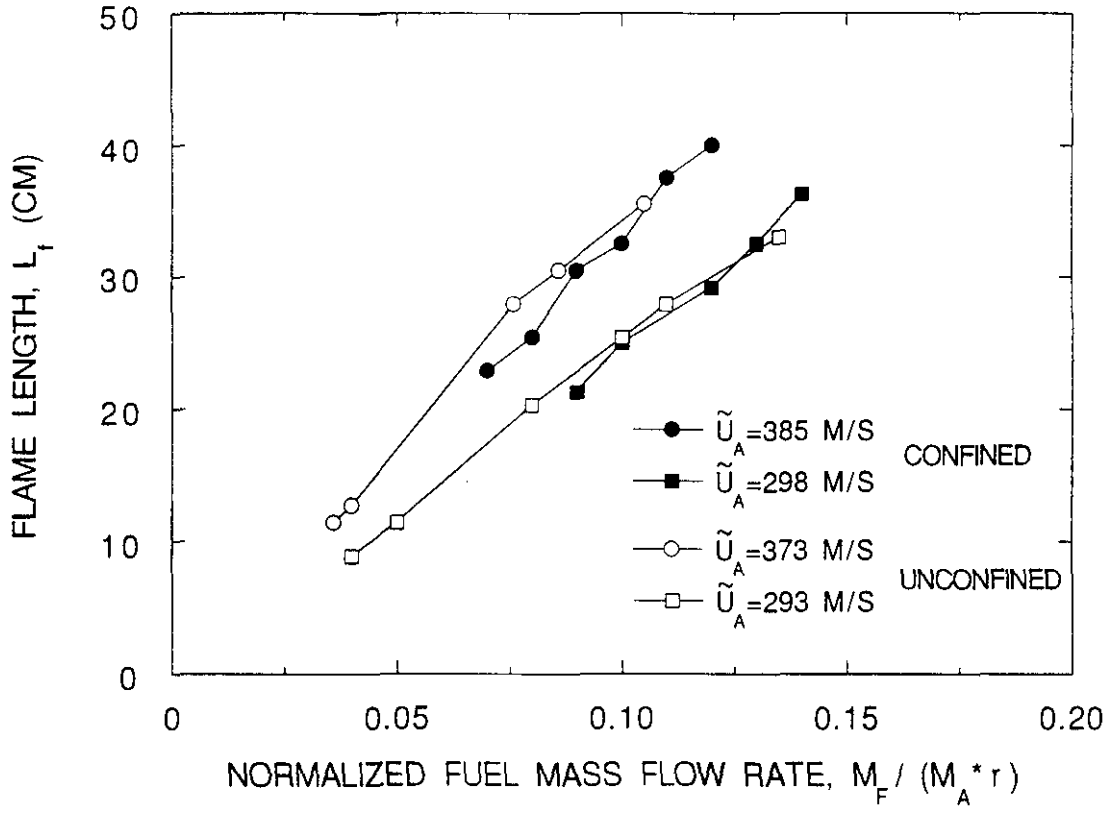

Figure 14. Measured Flame Length for Confined and Unconfined Cases. Air flow Mach number at fuel tube exit is 2.0. The stoichiometric fuel-air mass ratio is denoted r.